PHYSOR 2004 -The Physics of Fuel Cycles and Advanced Nuclear Systems: Global Developments
Chicago, Illinois, April 25-29, 2004, on CD-ROM, American Nuclear Society, Lagrange Park, IL. (2004)

Beam calculation for TRIGA reactor

Federico E. Teruel* and Rizwan-uddin
Department of Nuclear, Plasma and Radiological Engineering
University of Illinois at Urbana-Champaign
Urbana, IL 61801, USA

As part of the INIE project of the Big-10 consortium, efforts are underway at UIUC to assemble and test a set of codes that can be used for the design of the next generation of research reactor. SCALE 4.4 has been selected as one of the set of codes for this purpose. We here report some results of analysis of a TRIGA reactor using KENOVI, one of the codes in the SCALE system. Results are presented for a beam optimization study. Effects of several parameters on the level and spectrum of flux are reported.

KEYWORDS: TRIGA, thermal beam, SCALE, KENOVI

1. Introduction

The neutron flux inside a thermal beam depends on several parameters such us its geometry, its relative position in the reactor and other aspects that affect both the flux level and the flux spectrum delivered by the beam. Variation of the neutron flux, available flux level and spectrum as a function of this parameters provides data to characterization and optimization of thermal beams in a given reactor. The purpose of this work is to study the thermal neutron flux characteristics of a thermal beam placed in a TRIGA reactor as a function of beam's relative position, beam's geometry and relative position of external devices which modify the beam flux. In order to do so, several calculations have been performed to evaluate the dependence of neutron flux level, spectrum delivered by the beam, and the multiplication factor of the reactor on these parameters.

2. Reactor

The UIUC's TRIGA reactor, that has been in a SAFSTOR mode since 1999, has been chosen as a model to perform this study. Design data for a neutronics model of this reactor is available in [1].

The basic geometry of the TRIGA reactor is shown in Figure 1. The base configuration consists of a detailed core and a surrounding reflector without any facilities. The core is modeled as 126 holes or channels filled with 85 fuel elements (FE), 4 control rods (CR) and a central channel together with the remaining channels filled with light water. The maximum diameter of the core is 56.6 cm. The FEs are modeled with an external diameter of 3.75 cm and a height of 55.88 cm. The meat was considered fresh in all calculations and it was modeled as a mixture of 8 w% U in ZrH. The CRs were filled with borated graphite (B_4C), with natural concentration of B_{10}.

The reflector is composed of a cylindrical shell of graphite surrounding the core and two layers of light water at the bottom and top of the core. The cylindrical shell has the same height as that of the FE, and a diameter of 140 cm. A vacuum boundary condition is imposed at the outside surface of the reflector.

* Corresponding author, Tel. 217-244-7600, E-mail: teruel@uiuc.edu

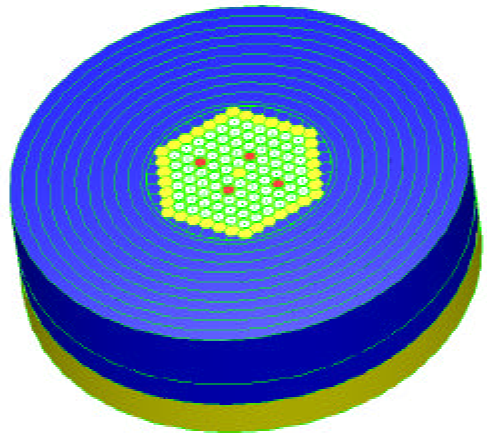

Fig.1 Bottom of the base model.

3. Neutronics Tool

The code selected to perform the calculations was KENOVI [2] which is one of the codes in SCALE 4.4 package (Standardized Computer Analyses for Licensing Evaluation) [3]. KENOVI is a Montecarlo code that allows modeling complex geometries and simulating neutron fluxes. The ability of KENOVI to handle a large variety of geometric shapes using combinatorial geometry makes it a useful tool to specify the problem geometry in great detail.

KENOVI can be run with different energy group structures and different libraries. Each library has been weighted with a particular neutron flux to represent a specific characteristic. The library chosen for the calculation was the 44-group ENDF/B-V [4]. This library contains more than 300 nuclides and it is developed by collapsing the 238GROUPNDF5 library also included in SCALE. This last library uses the same weighting spectrum for all nuclides. These are:

- Maxwellian spectrum (peak at 300 K) from 10E-5 to 0.125 eV ,
- 1/E spectrum from 0.125 eV to 67.4 KeV,
- fission spectrum (effective temperature of 1.273 MeV) from 67.4 KeV to 10 MeV,
- 1/E spectrum from 10 MeV to 20 MeV.

The 44-goup library has been tested and yields acceptable results for thermal systems [4]. The group distribution for the selected library is shown in Table 1.

Table 1 Library structure.

44-group library	Maximum Energy	Groups
Fast	20 MeV	12
Epithermal	0.1 MeV	20
Thermal	0.225 eV	12

The program was executed using 10,000 generation per case which yields acceptable errors in the thermal flux at the edge of the beam model. The number of neutrons per generation was 300 (default). No variance reduction technique was applied and the weight given to a neutron that survives the Russian roulette was 0.5. The starting neutron distribution was flat over the fissile material.

4. Beam Model and Results

The beam was modeled as a parallelepiped of fixed dimension with a square cross sectional area of 14 x 14 cm^2. In all cases, the beam has maximum length of 140 cm measured from the core center along its axis (i.e. the end of the beam is located at 140 cm from the core center, Figure 2). The beam is filled with helium at normal density. The relevant parameters to study in all cases are: the negative reactivity introduced by the beam with respect to the base case (i.e. without facilities), the neutron flux level and spectrum delivered by the beam at a fixed distance from the center of the core, and the rate at which the flux near the end of the beam changes.

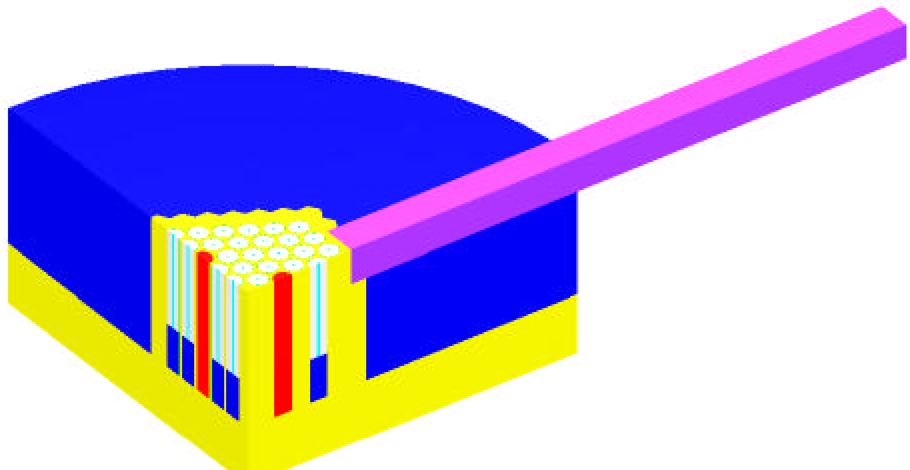

Fig.2 Radial beam model.

Each variation in the model introduces changes in the multiplication factor of the system. Therefore, all the fluxes were normalized with this factor to make the comparison between different cases possible. Further normalizations were introduced to set the power level of the reactor at 1.5 MW, which is the nominal power of the reactor modeled.

Fast, epithermal and thermal fluxes inside the beam corresponding to the model in Figure 2 are shown in Figure 3. In this case, the beam position is measured from the center of the core. The boundary of the reflector (70 cm) is clearly noted in the flux profile shown in Figure 3. The neutron flux along the beam was calculated in cells with the cross sectional area of the beam and 5 cm in length in all cases.

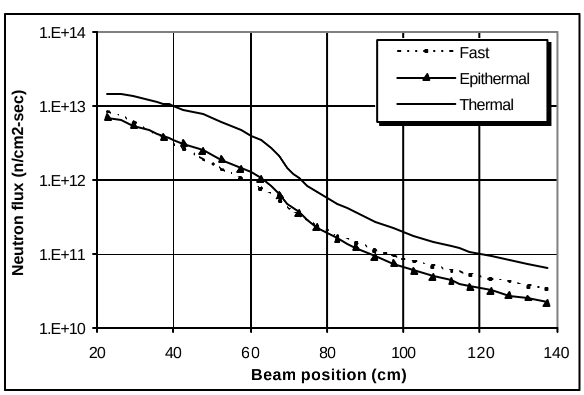

Fig.3 Typical neutron flux distribution along the radial beam.

Details of the flux levels in the UIUC's TRIGA reactor are not available. However, reference [1] gives 1.6E13 n/cm^2-sec as an expected average thermal flux in the FEs. In the calculations performed here, values of 2.7E13 n/cm^2-sec, 1.46E13 n/cm^2-sec and 1.09E13 n/cm^2-sec were respectively calculated for the thermal flux in the center water channel and in two particular FEs of the third and fifth hexagonal ring of the core. In addition, the thermal peak in the reflector was found to be 1.6E13 n/cm^2-sec (averaged in the meat FE's height, 39.1 cm).

4.1. Radial Beam Performance as a Function of Inlet Position

A radial beam was modeled with beam's inlet position as a parameter. Specifically, five models were developed in which the distance between the beam inlet and the center of the nearest fuel element varies from 3 to 9 cm (Figure 4) or from 22 to 28 cm from the center of the core. The first position was chosen inside the core area at 3 cm of the center of the nearest FE (R1 case), and four further positions were modeled moving the beam away from the core 1.5 cm at each step (R2 to R5 cases). The end of the beam is at the same point for all five cases. Assuming symmetry only a quarter of the core was modeled. Reflected boundary condition was imposed on symmetry planes. The goal of this calculation is to find the thermal neutron peak to place the beam's inlet plane and thus maximize the thermal flux in the beam.

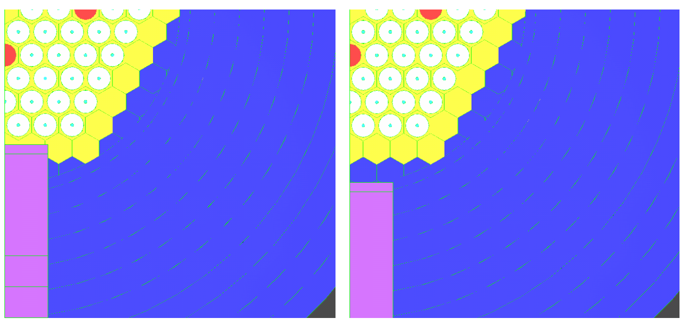

Fig.4 R1 and R5 cases.

To compare the results for different inlet positions, the thermal flux inside the beam is plotted in Figure 5. Each box shows thermal fluxes at different position along the beam. The first one corresponds to the beginning of the beam, the second one to a middle position and the last one to the model boundary. The error bars represent statistical errors and they are no greater than 7% for the fluxes at the boundary.

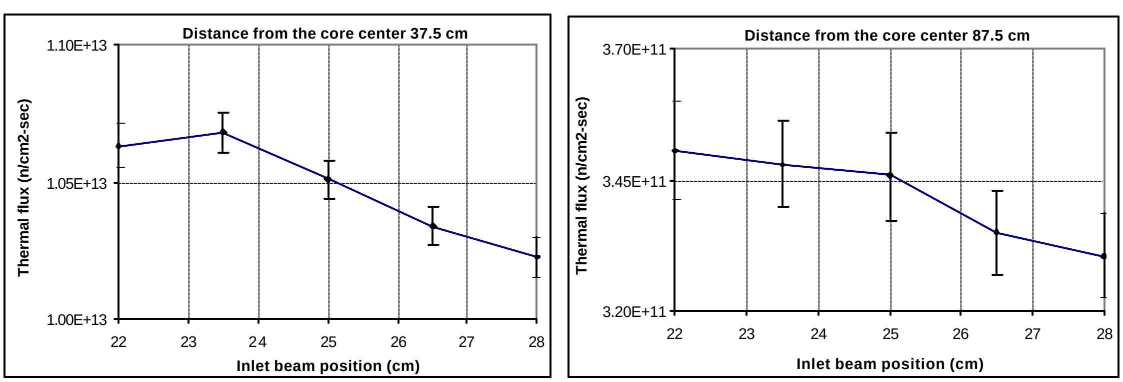

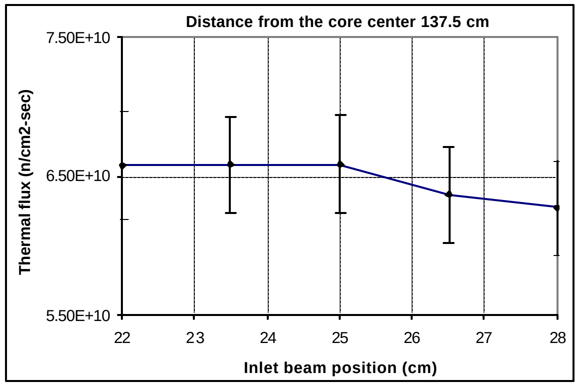

Fig.5 Thermal flux variation vs. inlet beam position for radial beams.

Figure 6 shows the reactivity changes introduced by the beam with respect to the base case. The behavior of this integral parameter is important because it allows comparing the hypothetical loss of reactivity against a hypothetical gain of flux. In addition, it indicates a perturbation in the core thermal flux that may result in a more inhomogeneous burn up of the FE located near the beam inlet.

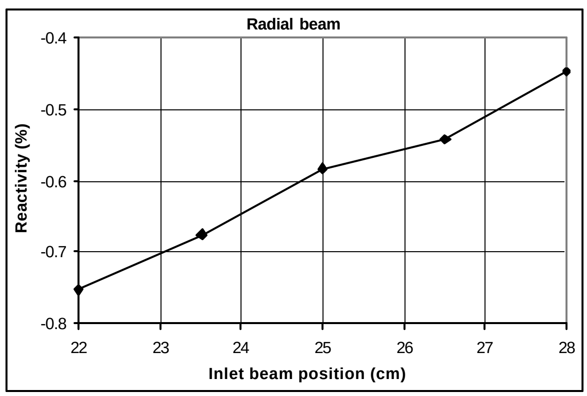

Fig.6 Reactivity changes as a function of the inlet beam position for radial beams.

The thermal spectrums for R1 and R5 cases at the edge of the model (or at a distance of 137.5 cm from the core center, which is the center of the outer cell modeled) are presented in Figure 7. Although a slightly more thermalized spectrum results for the R5 case, spectrums for these two cases are similar suggesting that the neutron thermalization is almost complete for all cases (i.e. R1 to R5). According to the Maxwellian distribution and the temperature selected for these calculations (50 °C), the thermal peak must be located at approximately 0.028 eV [5].

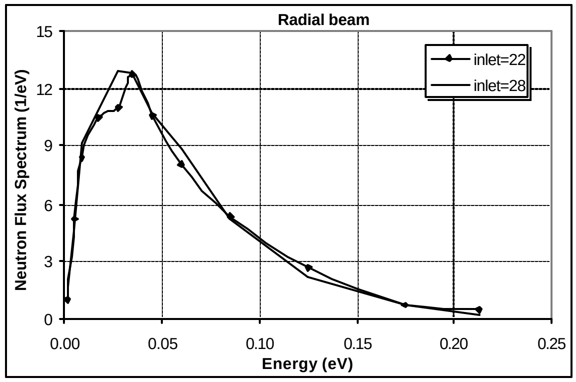

Fig.7 Thermal spectrums for R1 and R5 cases at the beam exit.

One parameter that characterizes the thermal neutron flux along the beam is given by the rate of drop of thermal flux along the beam. This parameter is related to the neutrons that have the beam direction and would contribute to the neutron flux further along the beam (without considering neutron guides). This drop can be calculated by fitting the flux with a power law, as is shown in Figure 8. The results are shown in Table 2 (all the correlation coefficients are greater than 0.999, however the statistical errors in the calculated fluxes are not considered in the calculation of this coefficient).

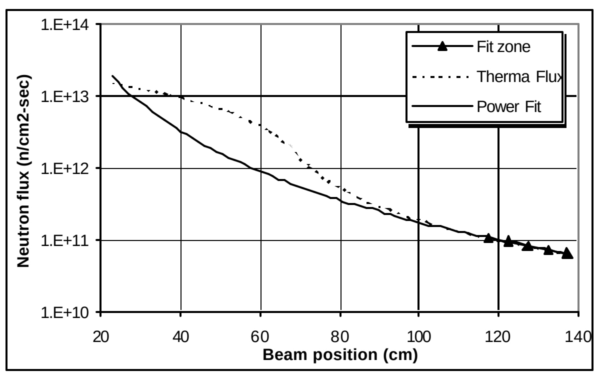

Fig.8 Power law fit over the thermal flux at the beam's end.

Table 2 Slope of the power law fit to the thermal flux at the end of the radial beam.

Case	Slope
R1	-3.16
R2	-3.15
R3	-3.17
R4	-3.21
R5	-3.10

Results suggest that the thermal neutrons, which leave the core to enter the beam, are essentially thermalized. Locating the inlet of the beam between 3-6 cm from the nearest FE keeps the flux level at maximum values without significant changes in the spectrum and without significantly affecting the flux drop inside the beam. Therefore, the position that produces the acceptable neutron flux level and reduces the negative reactivity introduced by the beam gives the most desirable position.

4.2. Tangential Beam Performance as a Function of the Inlet Position

The same beam geometry described earlier was modeled as a tangential beam. The inlet position was chosen again as a parameter to study the thermal flux in the beam. Four cases were studied, positioning the inlet of the beam at the core vertical centerline for the first model and moving 3 cm further away from this line for each successive model (T1 to T4 cases, Figure 9). In all cases the end of the beam was kept fixed at 140 cm (as in case T1). Symmetry was assumed, and hence only half of the core was modeled. Reflected boundary condition was imposed on the symmetry plane.

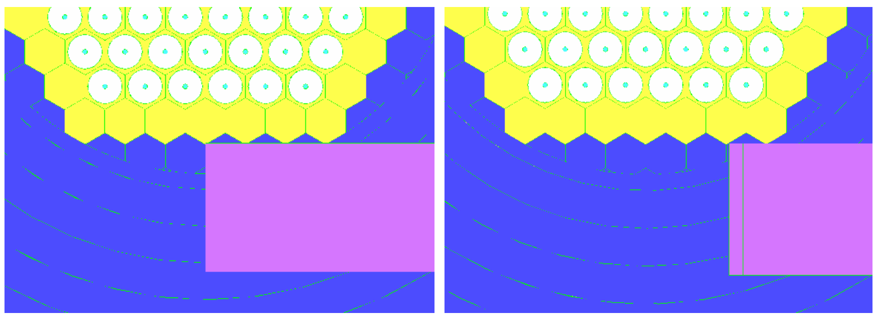

Fig.9 T1 and T4 cases.

Figure 10 shows the thermal fluxes at the middle of the beam and at the boundary of the model. The fluxes show similar drop with distance to the core centerline. The beam distance is measured from the core centerline which is perpendicular to the beam direction in the horizontal plane.

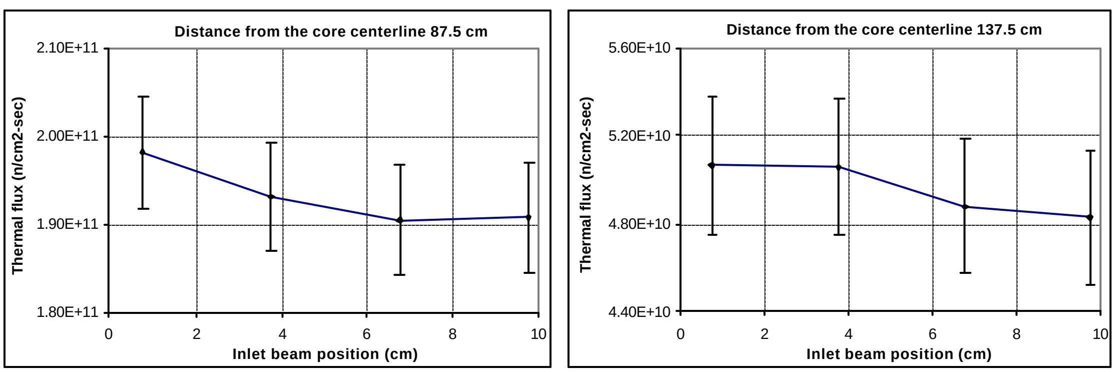

Fig.10 Thermal flux variation vs. inlet beam position for tangential beams.

The tangential beam models also introduce significant reactivity changes in the reactor. Figure 11 shows these variations for the four models.

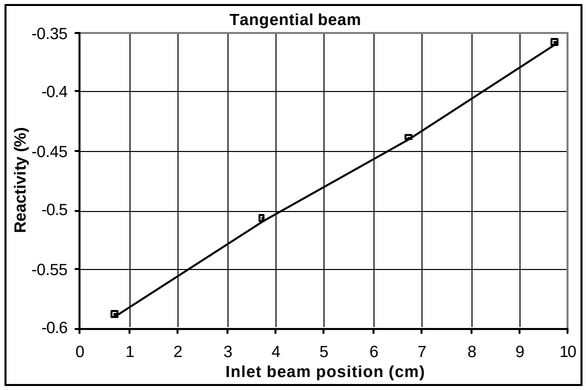

Fig.11 Reactivity changes as a function of the inlet beam position for tangential beams.

The thermal spectrum at 2.5 cm from the end of the beam (center of the outer beam's cell), is shown in Figure 12 for T1 and T4 cases, showing similar characteristics as the one in the radial case. A slightly more thermalized spectrum results for the T5 case.

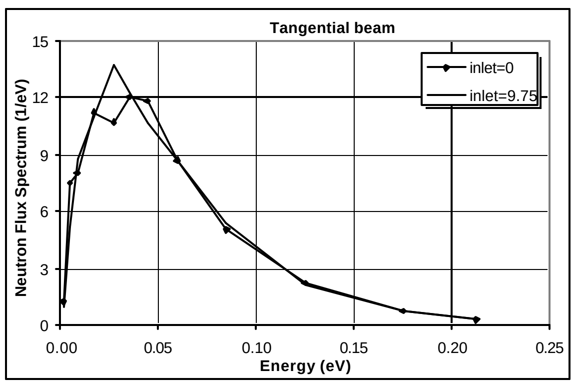

Fig.12 Thermal spectrums for the T1 and T5 cases at beam exit.

As for the radial beam case, thermal flux variation near the beam's end was fitted with a power law for each model. The values are presented in Table 3 showing a slower drop than the one for the radial beam case (all the correlation coefficients are greater than 0.998, however the statistical errors in the calculated fluxes are not considered in the calculation of this coefficient).

Table 3 Slope of the power law fit to the thermal flux at the end of the tangential beam.

Case	Slope
T1	-2.57
T2	-2.67
T3	-2.69
T4	-2.65

4.3. Radial Beam Performance as a Function of the Inlet Cross Section

Neutron flux in the beam can be increased by decreasing the beam width at the inlet and hence increasing moderation in this region. Five cases were studied using a radial beam with its inlet width in the horizontal plane as a parameter and maintaining its height constant and equal to 14 cm in all cases (Figure 13). These cases, S1 to S5, were characterized by inlet width of 4, 6, 8 10 and 12 cm, respectively. The inlet beam position was chosen as in the R2 case which has an inlet width of 14 cm. The outlet width was kept in all cases equal to 14 cm at the exit of the beam (i.e. at 140 cm from the core center). Assuming symmetry a quarter of the core was modeled. Reflected boundary condition was imposed on symmetry planes.

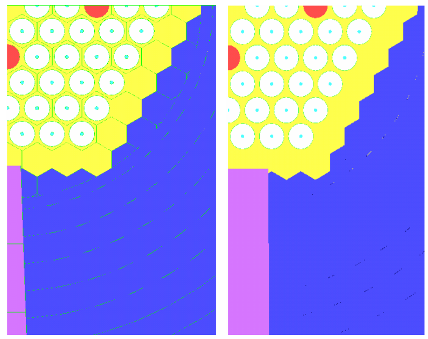

Fig.13 S1 and S5 cases.

The reactivity changes for the five cases are compared to the R2 case in Figure 14 (i.e. the base multiplication factor is taken from the R2 case).

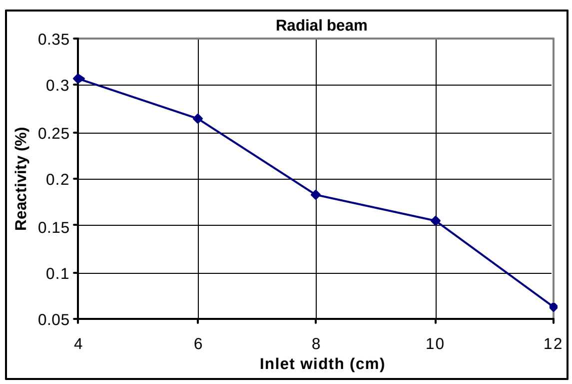

Fig.14 Reactivity changes decreasing the inlet width of R2 case.

Although moderation increases with inlet width reduction, as it is reflected in the reactivity plot and in the thermal flux ratio at the beam inlet (Figure 15), the thermal flux at the middle and end of the beam decreases with respect to the R2 case.

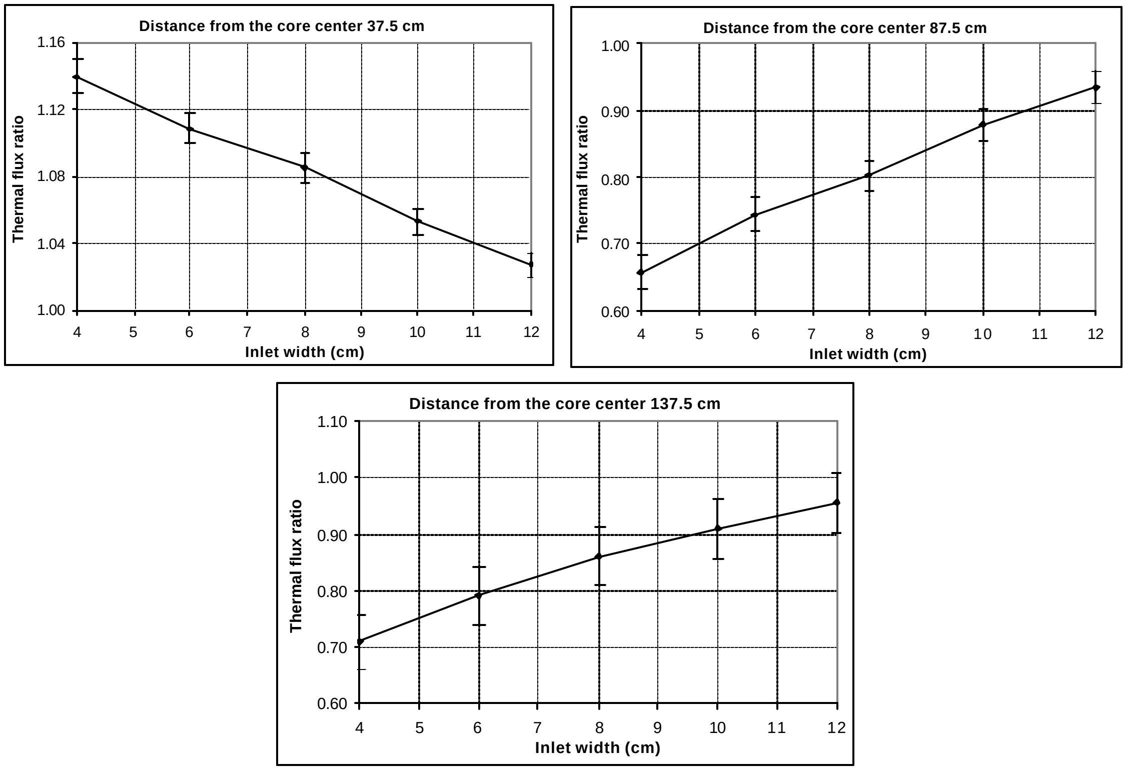

Fig.15 Ratio of he thermal flux for the S1-S5 cases and R2 case.

Again, the slopes were calculated for all the cases (Table 4), resulting in values similar to the ones calculated for the radial beam model (all the correlation coefficients are greater than 0.997, however the statistical errors in the calculated fluxes are not considered in the calculation of this coefficient).

Table 4 Slope of the power law fit to the thermal flux at the end of the beam.

Case	Slope
S1	-3.20
S2	-3.08
S3	-2.98
S4	-3.11
S5	-3.17

4.4. Performance as a Function of Beam Angular Position

Keeping the position of the center of the beam inlet fixed in the horizontal plane, the thermal flux behavior was studied considering dfferent angular beam positions. Four cases were studied. These are characterized by angular rotations in the horizontal plane with respect to the horizontal axis of 0, 30, 60 and 90 degrees (Figure 16). Assuming symmetry only half of the core was modeled. Reflected boundary condition was imposed on the symmetry plane.

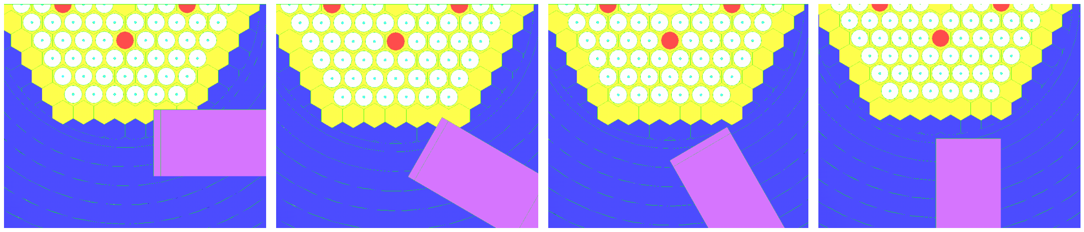

Fig.16 Beams with 0, 30, 60 and 90 degrees of angular positions.

The reactivity variation and the flux along the beams are plotted in Figure 17. In this case, it is interesting to note that the flux is highest for the tangential beam case which actually leads to the removal of a significant amount of moderator (or the negative reactivity introduced by the beam is greater). However the maximum flux for this tangential case is smaller than the one found for the R2 or R3 case. Also, the flux for the tangential case is higher than the radial one modeled here, because the proximity of the beam's inlet to the FEs contributes more to the beam's flux than the loss due to tangential orientation of the beam. In this case, the radial beam is 29 cm from the FE which is greater than the corresponding distance in the R5 case.

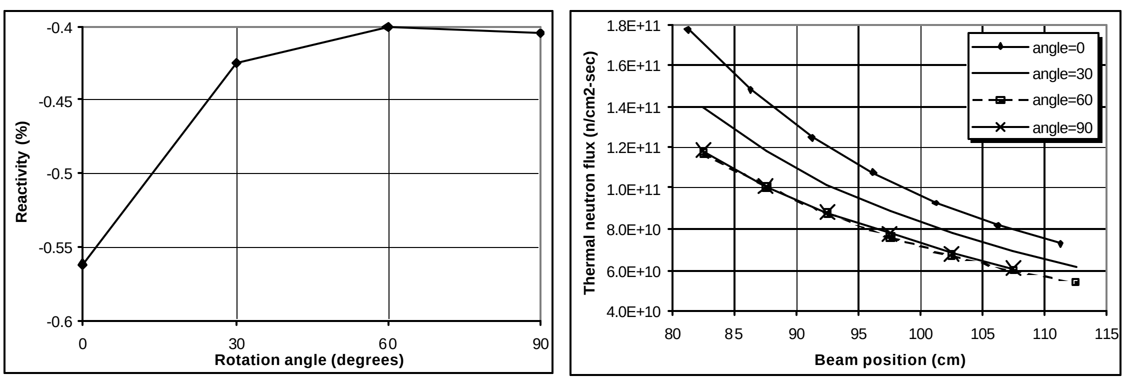

Fig.17 Reactivity variation and thermal flux distribution for the beams in different angular positions. An angle of zero degree corresponds to the tangential beam.

4.5. Effects of Device Interference on the Radial Beam Flux

Frequently, different devices have to be placed in the core reflector together with the beam. In cases where the proximity between the device and the beam inlet is close enough the device may affect the level and spectrum of the flux along the beam. To study this effect, a cylindrical device was modeled near the beam inlet. Three positions were modeled as shown in Figure 18 with two different materials: vacuum (cases V1-V3) and borated graphite as an absorber (cases A1-A3). The radial beam is located as in the R5 case. The cylinder is 15 cm in diameter and 14 cm high. The cylinder is almost touching the beam in the first case (position 1) and is moved by 5 cm each along a line parallel to the x axis for positions 2 and 3. Symmetry was assumed in vertical planes defined by the x and y-axis and thus a quarter of the core was modeled. Reflected boundary condition was imposed on these planes.

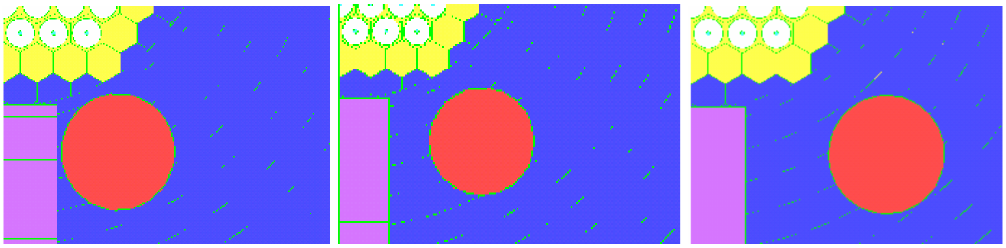

Fig.18 Geometry of the cylinder in positions 1, 2 and 3 respectively.

The reactivity variation for these six cases is presented in Figure 19. Here, the R5 case was taken as the base case. Therefore, the reactivity variations were calculated with respect to the multiplication factor of R5 case.

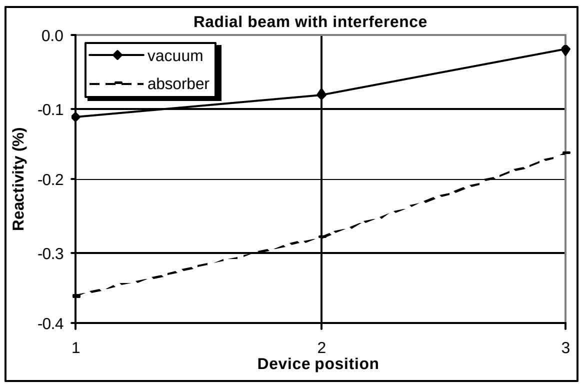

Fig.19 Reactivity variation for the vacuum and absorber cylinders at three different locations.

The thermal flux for these cases at two different positions in the beam are shown in Figure 20 together with the corresponding value for the R5 case (this value is placed at the device position 2 to facilitate comparison). For the vacuum cylinder the flux level is very close to the one without the device, however in the absorber case the flux level shows significant reduction. On the one hand, this shows that a strong absorber may introduce a significant drop in the flux level at the beam inlet. And, on the other hand, a weak thermal absorber may not produce a significant reduction in the flux level.

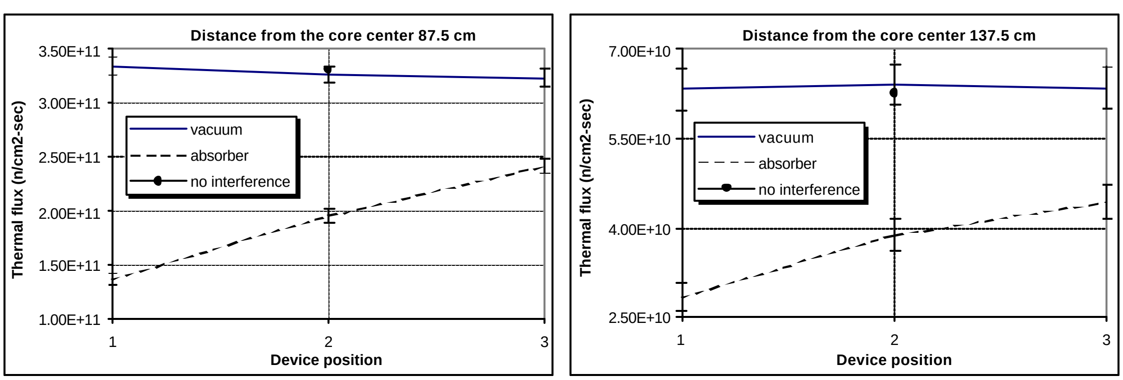

Fig.20 Thermal flux distribution along the beam.

Figure 21 shows the thermal spectrums for the cases V1, A1 and R5. The R5 and vacuum cases yield similar spectrums. Nevertheless, the case with a thermal-absorber device shows a depression at the energy that corresponds to the peak in the other two cases. As it was expected, the interference in the spectrum due to neutron absorbers may be significant and have to be taken into account especially when the utilization of the beam is focused on a part of its spectrum.

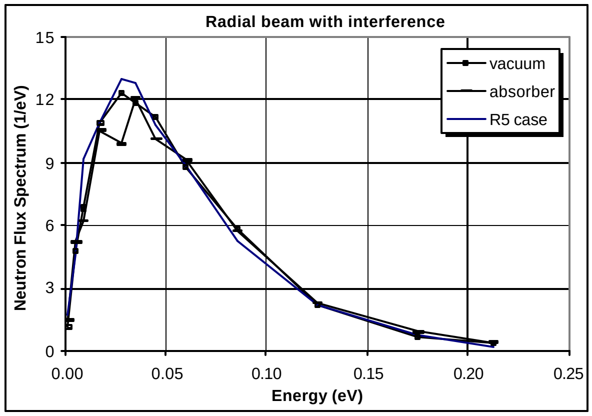

Fig.21 Flux spectrums with and without device interference.

5. Conclusions

The design of the TRIGA reactor core has not been optimized for beam lines. It is not a compact core with high neutron leakage. Therefore, the neutrons that leave the core and enter the beam are essentially thermalized. Analysis shows that the position of the beam inlet, which maximizes the thermal flux level, is only a couple of centimeters from the core face.

The maximum thermal flux level was found for the radial beam model with a value of 6.59E10 ± 7% n/cm^2-sec at 137.5 cm from the core center. The inlet position of the beam for this case is between 3 and 6 centimeters from the center of the nearest FE. The tangential beams present maximum fluxes of the order of 5.07E10 ± 7% n/cm^2-sec at approximately the same distance from the core (or 137.5 cm from the vertical core centerline). However, despite the difference in the flux level, the tangential beams are frequently preferred over the radial ones because they lead to lower non-desirable or secondary radiation.

The rate of decreasing flux along the beam shows an important difference between the radial and tangential beams. The latter one presents smaller leakage rate. This parameter must be taken into account in cases where the fluxes are required at distances larger than those modeled in these cases.

Decreasing the width of the beam inlet, results in a drop in the thermal neutron flux level at the beam exit. Although this leads to an increase in the neutron flux at the beam's inlet, the number of neutrons that enter the beam with the appropriate direction is drastically reduced.

In parametric study of beam orientation, as well as in the rest of the cases studied, the increase in the negative reactivity introduced by the beam orientation is followed by an increase in the neutron beam flux level (at least up to the distances modeled). This suggests the possibility to characterize the flux level along the beam using reactivity variations in cases where preliminary calculations are needed or when Montecarlo codes are not available to model the beam properly.

Neutron flux along the beam is only slightly affected by the presence of non-thermal absorber materials placed near the beam inlet. However, strong thermal absorber can reduce drastically the flux level along the beam even when they are located at considerable distance from the beam inlet.

This study, carried out using KENOVI of the SCALE family, allowed characterization of the neutron flux level and spectrum delivered by a thermal beam placed in a TRIGA reactor. The neutron flux variation was studied as a function of different parameters yielding a better understanding of the problem and making it useful in cases where different constraints on placement of the beam in the reflector are present.

6. References

1) G. P. Beck, "Safety Analysis Report for the Illinois Advanced Triga", University of Illinois at Urbana. Champaign, (1967).
2) D. F. Hollenbach, L. M. Petrie and N. F. Landers, "KENO-VI: a general quadratic version of the KENO program", ORNL/NUREG/CSD -2/V2/R6, Oak Ridge National Laboratory, (2000).
3) SCALE homepage, http://www.ornl.gov/sci/scale/.
4) W. C. Jordan and S. M. Bowman, "Scale Cross-Section Libraries", ORNL/NUREG/CSD-2/V/R6, Oak Ridge National Laboratory, (2000).
5) J. R. Lamarsh, "Introduction to Nuclear Engineering", Addison-Wesley, Philippines, 31 (1975).